

## T.4: Development and deployment of radiation resistant GaAs based PIN photodetectors

V. K. Dixit<sup>1</sup> and T. K. Sharma

Semiconductor Materials Laboratory

Materials Science Section

<sup>1</sup>Email: dixit@rrcat.gov.in

### Abstract

Radiation hard photodetectors are important for various applications in the harsh environment of high temperature, high pressure, and high radiation zones. In this context, the technology for the fabrication of radiation hard GaAs based p-i-n (PIN) photodetectors has been developed at RRCAT. The devices work in the wavelength range of 325 to 870 nm with a maximum responsivity of  $\sim 0.58$  A/W along with a dark current of  $< 1$  nA and can detect very weak signals of 2 nW power. Recently, a few customized detector systems are deployed in field applications, where photodetectors and necessary front-end electronics are made as per the user requirements. An early arc detection system as a safety device is deployed in an indigenously developed radio frequency circulator at RRCAT. Further, a dual element photodetector unit, consisting of two identical photodetectors on a chip, is developed for laser spectroscopy experiments at RRCAT. Radiation hardness of GaAs photodetectors is tested by exposing the devices to  $^{60}\text{Co}$   $\gamma$ -radiation sources and is found to be an order of magnitude higher when compared with commercially available silicon photodetectors.

### 1. Introduction

Semiconductor photodetectors are an integral part of several complex systems and find many interesting applications in the modern life [1-2]. In these devices, the detection of photons is governed by an effective collection of photo-generated electron-hole pairs [3-4]. An illumination of a semiconductor material with photons having energy larger than the bandgap injects electrons in the conduction band while leaving a hole in the valence band. Subsequently, the photo-generated electrons and holes drift in opposite directions under the influence of either built-in (internal) or external electric field. Separation of electrons and holes via this process gives rise to current flow across the device in a closed-circuit configuration. Here, the magnitude of photo current depends on the intensity of photon flux, absorption coefficient of semiconductor material, and quantum efficiency of the device. In order to have an internal built-in electric field, several configurations of the structures are being used. Semiconductor photodetector structures are designed and developed in many configurations such as Schottky, *p-n* and *p-i-n* (PIN) junction etc. The advantage of PIN junction configuration is associated with a large

depletion width, which results in higher quantum efficiency. A wide depletion region leads to relatively small capacitance which results in high bandwidth of detection. Semiconductor junctions are engineered via an extreme control of dopant density profile during the epitaxial growth. Out of all the semiconductor materials, III-V compound semiconductors have been used to develop key optoelectronic devices for a variety of conventional and advanced applications over a wide wavelength range varying from infrared to x-ray region [3-10]. A few latest breakthroughs have spurred the development of novel devices by keeping a major focus on the improvement of peak responsivity, and also the radiation hardness. GaAs, CdTe, InP, GaN, SiC semiconductor materials offer higher radiation tolerance against  $\gamma$ -rays, electrons, protons, and neutrons and can work in harsh environments over extended durations [7-19] as compared to Si or Ge. However, in India, fabrication of compound semiconductor devices is limited to a few R & D labs and a majority of these devices are being imported even today. Semiconductor Materials Laboratory at RRCAT have been working in this area for the last two decades where a major emphasis is given on R&D of advanced light emitters and detectors based on conventional group III-V and III-N compound semiconductors. In this article, salient features of the fabrication technology of GaAs based PIN photodetectors are described including the relevant basic physics. Key parameters asserting the state-of-the-art performance of indigenously developed devices are also reported. Representative applications of the devices are highlighted by providing results from a few experiments. Details of a few customized detector systems that are fabricated as per the user requirements are also given. Radiation hardness of these devices against the exposure to  $^{60}\text{Co}$   $\gamma$ -radiation sources is also discussed.

### 2. Experimental details

Fabrication procedure of GaAs based PIN photodetectors is described in this section. It includes epitaxial growth of multilayer structure, and various devices fabrication steps like photolithography, metallization, device isolation, passivation, annealing, wire bonding, packaging, and device testing.

#### 2.1 Layer structure and growth conditions

The typical layer structure of PIN photodetector consists of an undoped 5.5  $\mu\text{m}$  thick intrinsic (i-type) layer of GaAs sandwiched between 20 nm of p-type ( $\sim 2 \times 10^{18} \text{ cm}^{-3}$ ) and 600 nm of n-type ( $1 \times 10^{18} \text{ cm}^{-3}$ ) GaAs layers as shown in Figure T.4.1(a). Numerically calculated energy band profile of the photodetector structure is shown in Figure T.4.1(b). In a few devices, internal gain layers are also embedded in the intrinsic region of device. GaAs based multilayer structures are

epitaxially grown by AIX-200 metal-organic vapor phase epitaxy (MOVPE) system on 2-inch diameter n<sup>+</sup>-GaAs substrates in the temperature range of 600-700 °C. Tri-methyl gallium and arsine are used as the precursors while silane and diethylzinc are used for n and p-type doping respectively. Each layer of the multilayer stack is individually optimized with respect to the dopant density, whereas crystalline quality is optimized by growing an undoped GaAs layer under different growth conditions. A few calibration growth runs are therefore needed prior to the epitaxial growth of complete PIN photodiode structure.

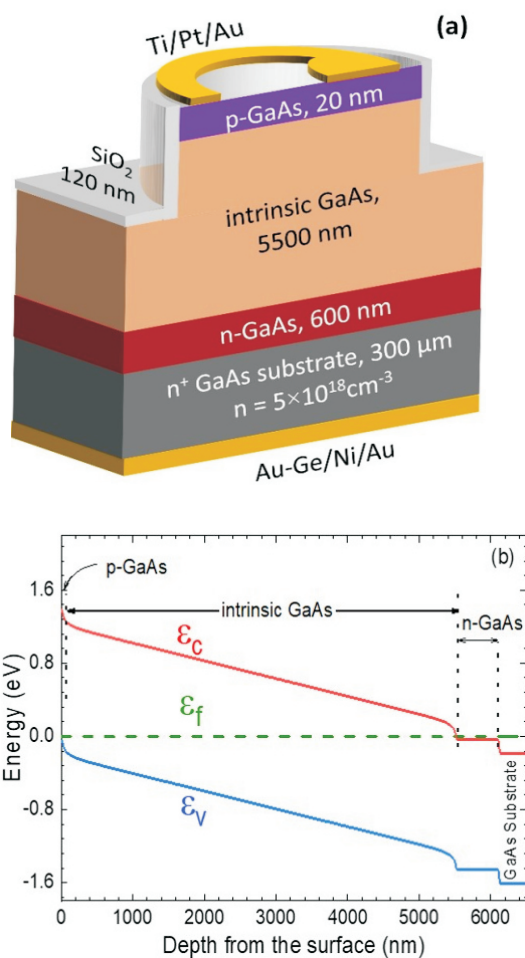


Fig. T.4.1:(a) Schematic cross sectional view, and (b) energy band profile of GaAs p-i-n photodetector.

### 2.2 Device fabrication

After epitaxial growth, fabrication of semiconductor photodetectors is performed by implementing several device processing steps. First, Au-Ge/Ni/Au multilayer contacts are

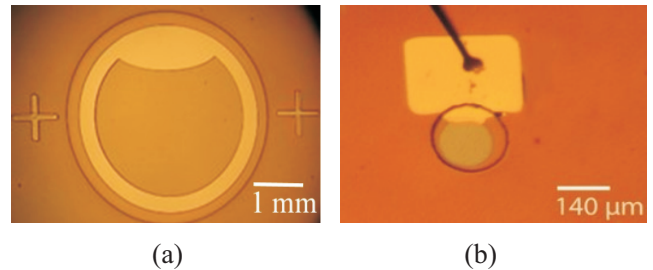


Fig. T.4.2: Photographs of GaAs photodetector element having a diameter of (a) 3 mm, and (b) 100 μm.

deposited on the backside of n<sup>+</sup>-GaAs substrate by thermal evaporation technique, which is then followed by rapid thermal annealing (RTA) at 375 °C for 45 s under nitrogen environment. Second, the active area of photodetector is defined through photolithography step. Here, photoresist (Shipley S1813) is coated on the top of epitaxial structure with the help of a spin coater. The sample is then exposed to an ultra-violet beam for a given duration which is then processed for defining the active area of device. Third, a controlled chemical etching of epitaxial structure is performed by dipping the sample in CH<sub>3</sub>(OH):H<sub>3</sub>PO<sub>4</sub>:H<sub>2</sub>O<sub>2</sub> (6:3:1) solution for 10 s at 35 °C. It helps in defining the active area of device. Fourth, a layer of SiO<sub>2</sub> with thickness of ~120 nm is deposited on the sample by electron beam evaporation technique [20-22]. This helps in the passivation of surface states and also in minimizing the reflection of photons from the detector surface. Fifth, second photolithography step is performed to define the top-contact area. Sixth, selective area oxide removal is carried out by dipping the sample in buffer HF solution, which therefore provides direct access to p-GaAs layer in the defined region for the deposition of top-contact as shown in Figure T.4.1(a). Seventh, Ti/Pt/Au multilayers are deposited on the designed pattern on the top of the detector structure, which is then followed by a metal liftoff procedure and rapid thermal annealing. At the end of seventh step, fabrication of individual detector element is completed. Photograph of a large area photodetector element is shown in Figure T.4.2(a), while that of a 100 μm diameter one is shown in Figure T.4.2(b). Eight, the detector chip is die attached with the help of silver epoxy on Au-plated copper mounts, which provides the back contact. Ninth, 1 mil (~25 μm) thick Au wire is bonded to the front contact by ball-wedge bonding procedure. It completes the fabrication of photodetector device which is ready for mounting in specially designed detector headers as per the requirement of user. Photograph of 12 numbers of GaAs PIN photodetectors with size varying from 100 μm to 6 mm diameter is shown in Figure T.4.3. These detectors are mounted in the indigenously designed

device headers. Some of the fabrication steps had to be customized in order to meet the user requirements that often vary depending on the complexity of application. One critical step is to define the size of detector element which is application specific. For example, for low dark current applications, a small element size (100 μm or lower) is preferred. On the other hand, large area photodetectors are generally preferred by most of the users. In some cases, a very specialized geometry of detector element is preferred by the user. One such example from laser spectroscopy is discussed in the later part of the article. In conventional fabrication route, one requires a new set of masks for photolithography, whenever a change in the geometry of detector element is sought by the user. It is quite inconvenient, since it not only requires extra funds and time but also discourages newer developments. Keeping this in mind, a low cost mask-less photolithography setup is made and is currently being used in the development of novel semiconductor devices on routine basis. It is developed by using a digital-projector and a stereo-zoom optical microscope [23].



Fig. T.4.3: Photograph of 12 numbers of GaAs PIN photodetectors with element size varying from 100 μm to 6 mm diameter

### 2.3 Device testing

Operating performance of the devices needs to be checked through various characterization procedures before their deployment in field applications. Figure T.4.4 shows the representative current-voltage characteristics of a photodetector with 5 mm diameter which can be biased upto -40 V. For low dark current applications, a specific structure with internal gain is designed and the performance of such a device having 3 mm diameter is shown in the inset of Figure

T.4.4 [24]. It is obvious from the inset that the dark current increases from 5 pA to 2 nA under light exposure. It is also shown that the device can read laser power down to 2 nW.

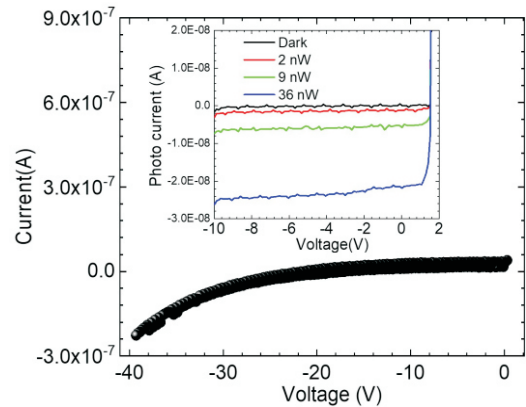


Fig. T.4.4: Current-Voltage characteristics of indigenously developed GaAs photodetector. Inset shows variation in the reverse saturation photocurrent of a specially designed device under light exposure at 730 nm.

Next, the responsivity (R) of photodetectors is estimated by using the relation,  $R=JA/P_{in}$ , where J is photocurrent density, A is area of detector element, and  $P_{in}$  is the power of incident light. Quantum efficiency ( $\eta$ ) and specific detectivity ( $D^*$ ) of the device are also estimated by using the following expressions [24-25];

$$\eta = \frac{Rhc}{e\lambda} ; \quad D^* = R \sqrt{1 / \left( \frac{4k_B T}{R_d A} + 2eJ_{dark} \right)}$$

where, h, c, e,  $\lambda$ , and  $k_b$  have their usual meaning,  $R_d$  stands for the dynamic resistance of device, T is temperature in kelvin and  $J_{dark}$  is the dark current at temperature T. It may be noted that the value of  $D^*$  might change slightly after including the generation–recombination process in the active region of the device. Further, the spectral response of photodetectors is shown in Figure T.4.5. The detector works in the wavelength range of 325 to 870 nm with a maximum responsivity of ~ 0.58 A/W at 869 nm and the dark current remains < 1 nA even for devices having large diameter approaching 10 mm. The operating characteristics of indigenously developed photodetectors are summarized in Table T.4.1. These are the best set of parameters achieved for the indigenously developed devices, which certifies a state-of-the-art performance of GaAs PIN photodetectors. It is needless to say that particular device characteristics can be fine-tuned as per the user requirement, including the range of spectral response, which can be tailored by growing a different heterostructure by MOVPE.

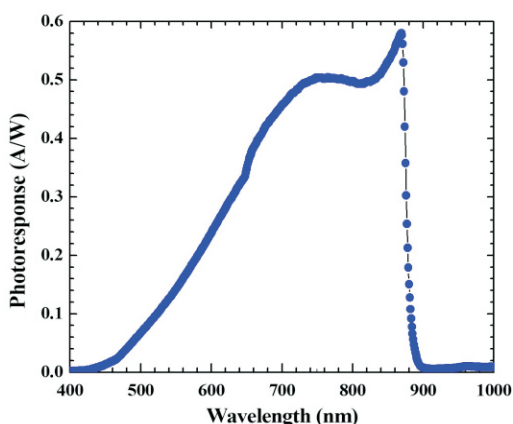


Fig. T.4.5: Spectral response of indigenously developed GaAs photodetector.

Table T.4.1: Operating characteristics of indigenously developed GaAs photodetectors.

Device parameter	Value
Spectral range	325 to 870 nm
Peak responsivity	0.58A/W at 869 nm
Quantum efficiency	84 %
Specific detectivity	$\sim 10^{13}$ (cmHz <sup>1/2</sup> W <sup>-1</sup> )
Rise time	2.5 nsec
Minimum detectable power	1.8 nW
Minimum dark current	5 pA
Operating voltage range	0 to -35 V
Diameter of element*	100 $\mu$ m to 10 mm

\* Diameter of detector element can be varied as per the user requirement.

### 3. Deployment of indigenously developed GaAs PIN photodetectors

Excellent operating characteristics of indigenously developed devices as shown in Table T.4.1 encouraged us to look for their possible applications in the departmental work. A brief summary of the deployment of indigenously developed GaAs PIN photodetectors is given in this section.

#### 3.1 Application in photoluminescence spectroscopy

Photoluminescence (PL) spectroscopy is a standard method to characterize the optical quality of epitaxial layers. A strong PL signal indicates better crystalline quality of the material under investigation. GaAs PIN photodetectors are used for measuring the PL spectra of various quantum well (QW) samples grown in our lab. Figure T.4.6(a) shows the schematic layer structure of a multi QW structure which is

used as a test sample. PL spectrum of this sample is recorded with the help of a commercially available Si photodetector, and also with an indigenously developed GaAs photodetector. The outcome of such an exercise is shown in Figure T.4.6. It certifies the usefulness of developed devices in PL spectroscopy.

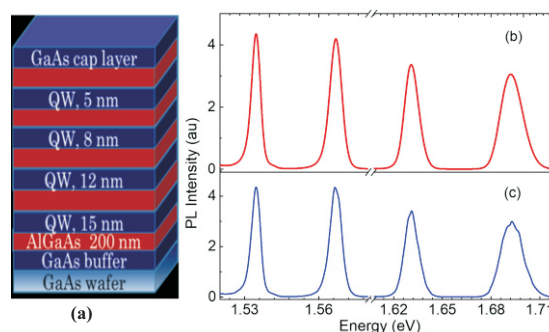


Fig. T.4.6:(a) Schematic layer structures of a multi quantum well structure, and PL spectra of sample recorded with (b) commercially available Si photodetector, (c) indigenously developed GaAs photodetector.

#### 3.2 Detection of degree of circular polarization of PL

Spin-photonics is another emerging area where indigenously developed GaAs photodetectors can play an important role. In these experiments, detection of the degree of circular polarization (DCP) of light emitted by QW samples is correlated with the density of spin-polarized electrons [26]. A major hurdle in such experiments is to detect a very weak spin-polarized PL signal, typically of few nW power. In such an experiment, strength of the signal is mainly governed by the spin relaxation mechanisms acting in the QW sample. One usually opts for a photomultiplier tube (PMT) for such sensitive measurements. Figure T.4.7 shows the outcome of such an exercise where DCP of a QW sample is measured with the help of a PMT and also by an indigenously developed GaAs photodetector.

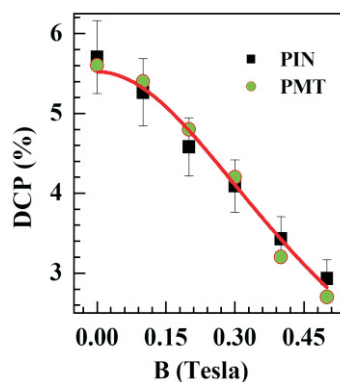
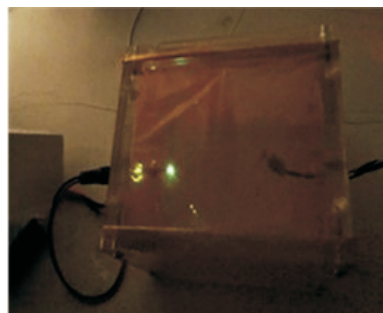


Fig. T.4.7: DCP of PL signal of a quantum well sample measured by using an indigenously developed GaAs photodetector and a PMT.

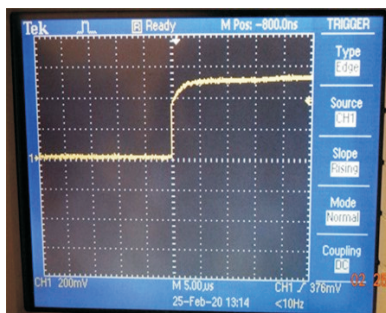
It is quite encouraging to see that the indigenous device can deliver the desired outcome even in such specialized experiments. From the magnetic field dependence of DCP, an electron spin relaxation time of 50 ps ( $\pm 3.5$  ps) is estimated. This also demonstrates the usefulness of indigenously developed detectors in the measurement of spin lifetime of charge carriers in a QW sample.

### 3.3 Arc fault detection system for RF circulator

Customized single element GaAs based PIN photodetectors are made for arc fault detection applications in radio frequency (RF) circulator systems. A quick response of the sensor is critical for this application. Keeping this in mind, the temporal response of indigenously developed photodetectors is measured by using femtosecond laser pulses and is found to be  $\sim 2.5$  ns. Initially, the performance of GaAs photodetector for safety operation is checked by developing a lab-based arc ignition facility. A photograph of this facility is shown in Figure T.4.8(a). Here, an arc is artificially generated for a pre-defined duration and the response of GaAs sensors is tested with respect to arc test pulse. One representative pulse recorded by the GaAs sensor is shown in Figure T.4.8(b). It can be seen that the sensor can read the arc pulse within a period of  $< 5 \mu\text{s}$ , which is sufficient for meeting the user requirements.



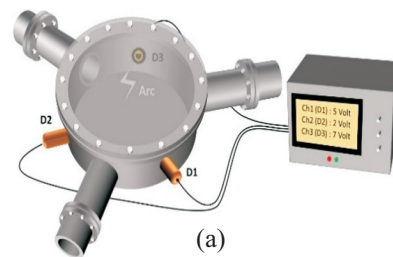
(a)



(b)

Fig. T.4.8: (a) Photograph of a test setup for arc fault detection. (b) Trace of an arc pulse detected by the GaAs sensor.

Next, an arc fault detection system is designed and developed by using a trans-impedance amplifier and GaAs PIN photodetectors. The system contains mainly three input channels for the connection of sensors and an LCD display to show the magnitude of signal corresponding to each sensor. A schematic diagram of arc fault detection system deployed in a RF circulator is shown in Figure T.4.9(a). Necessary mounts for holding GaAs photodetectors are also made as shown in Figure T.4.9(b). GaAs photodetector elements are placed at the tip of mount which has a BNC output connector at the other end. It is ensured that the detector assembly is compatible with RF environment. Further, the system contains a scaling circuit and STM-32 microcontroller for the digitization of analog signals and to display the digitized signal on a 20x4 LCD screen as shown in Figure T.4.9(c). This system continuously monitors the three sensors and triggers an alarm at a pre-settable value. Whenever an arc is detected by any of the three sensors, it generates an audible as well as visible alarm.



(a)



(b)



(c)

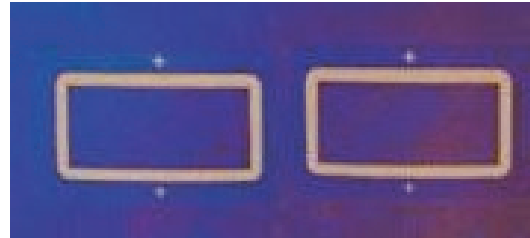
Fig.T.4.9: (a) Schematic diagram of arc fault detection system with three input channels, (b) photograph of an indigenously developed GaAs sensor for arc fault detection, and (c) photograph of the control panel of arc fault detection system.

Further, the safety system latches the alarm state until the same is cleared by the user. Potential free normally-closed contacts are provided to user as additional safety measure for shutting down the load in case an alarm is triggered. After a series of tests in lab, indigenously developed arc fault detection system is deployed in the RF circulator, developed by RFS, RRCAT which primarily works as a safety interlock for switching off the electrical supply as per the user requirement. The system is in regular use at RFS in RF circulator operating at about 40 kW power.

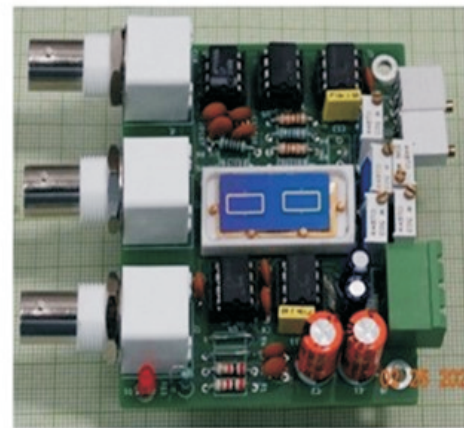
### 3.4 Balanced photodetector for laser spectroscopy applications

Balanced photodetectors find several interesting applications in laser spectroscopy. Here, one measures the difference in the intensity of two laser beams, which are of same intensity and a minor difference is caused by some physical phenomenon. In order to do this, a very sensitive detection unit is required by the user that is capable of measuring a very small difference in the intensity of two laser beams with a high signal-to-noise ratio. In view of this, balanced photodetectors are quite attractive since laser noise or any other common noise can be canceled out. This leads to the detection of a weak signal overriding on a large DC background. In a balanced photodetector, two photodetectors are connected in such a way that the effective output becomes zero, as long as the intensity of laser beams incident on the two detectors is same. This imposes a stringent condition to make the performance of two photodetectors almost identical. In order to achieve this, two identical GaAs based photodetectors ( $PD_1$  &  $PD_2$ ) are fabricated on a single chip as shown in Figure T.4.10(a). The detectors are of  $4 \times 7 \text{ mm}^2$  size along with a spacing of 3 mm as required by the user. A rectangular geometry of detector element is required to accommodate an elliptical laser beam as per the user requirement. Further, a large size of detectors is needed to minimize the error due to any minor displacement of the laser beam during the experiments. In order to minimize the noise, and also to keep the assembly compact, a special packaging is designed and developed as shown in Figure T.4.10(b). The dual detector chip is mounted on a PCB along with all the readout electronics. The photocurrent from  $PD_1$  and  $PD_2$  is amplified by LF356 operational amplifier based trans-impedance amplifiers which is further amplified by variable gain voltage amplifiers. The amplified signals are then processed through INA105 precision unity gain differential amplifier. The dual-element detector along with the electronics is packaged in a metal box and provision to read the output of individual detectors along with the differential signal is made available to the user. The performance of the complete system is tested by using a 633 nm He-Ne laser. The incident power ( $P_0$ ) on  $PD_1$  is fixed at  $95 \mu\text{W}$  and that of  $PD_2$  ( $P_0 + \Delta P$ ) is varied by using a circularly variable neutral density filter. The dual-element detector is

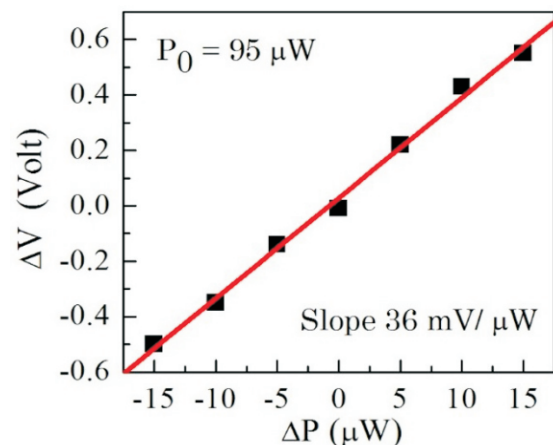
found to be extremely sensitive to the difference in incident power with a sensitivity of  $36 \text{ mV}/1 \mu\text{W}$  as shown in Figure T.4.10(c). It is important to note that such specialized balanced photodetectors are not commercially available.



(a)



(b)



(c)

Fig. T.4.10: (a) Photograph of dual element GaAs photodetector chip, (b) Photograph of balanced photodetector system, where dual element detector is mounted on top of PCB, (c) the differential signal generated ( $\Delta V$ ) as a function of difference in incident power ( $\Delta P$ ).

### 3.5 GaAs based x-ray detectors

GaAs photodetectors find interesting applications in x-ray region of electromagnetic spectrum due to their radiation hardness along with a high photon absorption efficiency when compared to silicon [8-10]. In view of this, prototype x-ray detectors based on GaAs materials are also fabricated. Such detectors operating in the range of 20–100 keV are attractive for medical imaging applications. Silicon detectors are not ideal for x-ray applications in 20–100 keV range since silicon has quite a low absorption above 20 keV. In view of this, GaAs based PIN photodetectors with very thin p-GaAs layer are specially grown. Photodetectors are fabricated and are successfully tested against laboratory based  $\text{CuK}\alpha$  x-ray source. The energy-dependent x-ray response of GaAs PIN detector is also measured by using a monochromatic x-ray beam with energy varying from 8 to 25 keV at BL-2 beamline of Indus-2 synchrotron radiation source as shown in Figure T.4.11. It confirms the suitability of indigenously developed GaAs detectors over a wide x-ray spectral range. Further refinements for enhancing the signal strength and also to widen the energy range are in progress.

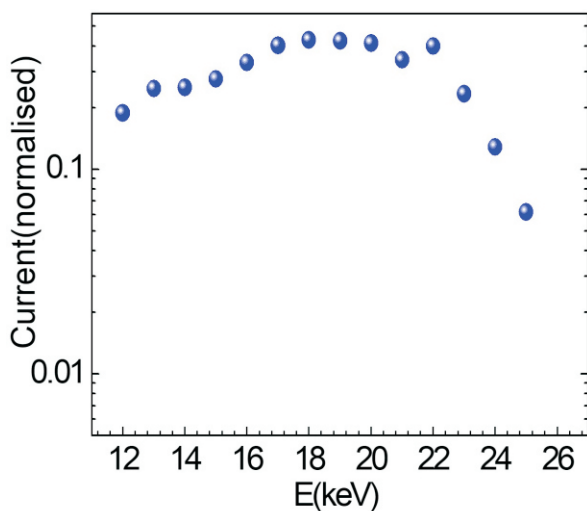


Fig. T.4.11: Spectral response of indigenously developed GaAs based x-ray detector recorded at BL-2 beamline of Indus-2.

### 4. Radiation hardness of indigenously developed GaAs based PIN photodetectors

GaAs is expected to be radiation hard when compared with commercially available silicon photodetectors. In view of this, GaAs photodetectors were exposed to 360 kGy of  $\gamma$ -radiation [23-25]. All the irradiations were performed at room temperature in a 2490 Curie  $^{60}\text{Co}$  gamma chamber (Model No; GC-900) supplied by the Board of Radiation and Isotope

Technology, Mumbai. After the exposure of GaAs detectors to  $\gamma$ -rays, an increase in the dark current per unit volume ( $J_v$ ) is seen as a function of  $\gamma$ -ray fluence ( $\Phi$ ) as shown in Figure T.4.12. The slope ( $\alpha = \Delta J_v / \Delta \Phi$ ) of the current per unit volume versus  $\gamma$ -ray fluence is estimated to be  $\sim 5 \times 10^{-19}$  A/cm for GaAs which is lower by an order of magnitude when compared to Si. A lower value of  $\alpha$  confirms that radiation tolerance of GaAs is more than that of Si, particularly in the high flux  $\gamma$ -ray environment. Results shown in the inset of Figure T.4.12 confirm that there is a significant recovery of the radiation damage as the time elapsed after the irradiation. Such an improvement is predominantly due to the reduction of carriers contributing to the saturation current. Thus, it is proven that the radiation induced defects can be partially recovered even without any high temperature annealing step [27-29]. Such a self-recovery of GaAs based devices is really attractive. Due to such attributes, GaAs based detectors are attractive for many applications in high temperature, high radiation zones, for example direct electron detection spectrometer, and also for space science missions [30-32].

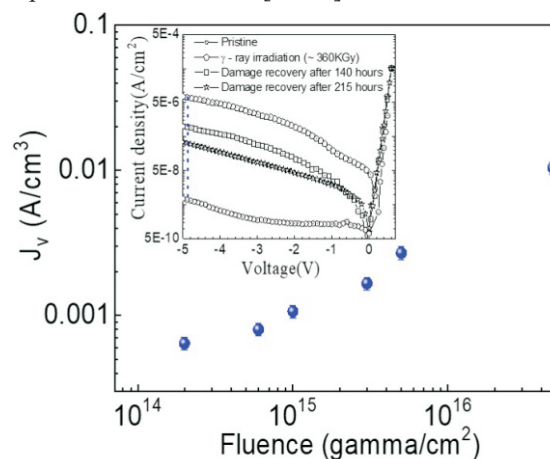


Fig. T.4.12: Reverse saturation current per unit volume as a function of irradiated dose, inset shows the recovery of radiation induced damage as a function of cumulated annealing time at RT.

### 5. Conclusion

A complete technology for the fabrication of GaAs based photodetectors is developed. It involves design and multilayer growth by MOVPE technique and various devices fabrication steps that are needed for the fabrication of GaAs detector chips. The fabrication steps are also optimized for customized applications. Thereafter, GaAs based photodetectors are used in spectroscopy experiments to record the PL spectra of various QW samples. Performance of GaAs based detectors is found to be similar to that of commercially available silicon photodetectors. GaAs based photodetectors are found

suitable to replace the PMT in low noise applications for measuring the DCP of PL signal emitted by a QW sample. An arc fault detection system based on GaAs photodetectors is also developed and is deployed in RF circulator as a safety system to switch off the load in case an arc is detected. A balance photodetector assembly is developed by incorporating a custom built dual detector chip for interesting applications in laser spectroscopy. GaAs based x-ray prototype detectors are also made which works in the energy range of 12 to 25 keV. It demonstrates our capabilities for the development of customized radiation hard photodetectors based on GaAs epitaxial layers. Development of a few more customized semiconductor photodetectors as per the needs of RRCAT users is in progress. Finally, the radiation tolerance of GaAs photodetectors is measured by exposing the devices to 360 kGy of  $\gamma$ -radiation. The devices were found to be operational even after exposure to such a high dose and their radiation tolerance is found to be an order of magnitude higher when compared with commercially available silicon photo detectors. The technology developed here can find several interesting applications in the harsh environment of high temperature, high pressure, and high radiation zones.

#### Acknowledgement

In this article, we have summarized the work which has been carried out by the entire team of Semiconductor Materials Laboratory during the last few years and their contribution is hereby acknowledged. We acknowledge the colleagues from RFSD, LPAS, SUS, FSOSS, LCID, Laser Workshop and Chemical Treatment Laboratory, who had made useful contributions. In particular, Dr. Ashish Kumar Tiwari, RFSD, Dr. S. P. Ram, LPAS, and Dr. S. K. Rai, SUS contributed in the development of customized devices. Authors would like to thank Shri S. V. Nakhe, Director, Materials Science Group and Shri Debashis Das, Director, RRCAT for their constant support and encouragement.

#### References

- [1] P. M. Johns and J. C. Nino, "Room temperature semiconductor detectors for nuclear security," *J. Appl. Phys.*, 126, 040902, (2019).
- [2] M Rizzi et al, "Semiconductor detectors and principles of radiation matter interaction," *J. Appl. Sci.*, 10, 3141 (2010).
- [3] V. K. Dixit, S. K. Khamari, C. Tyagi, S. D. Singh, S. Porwal, R. Kumar, C. Mukherjee, P. Mondal, A. K. Srivastava, T. K. Sharma and S. M. Oak, "Evaluation of electronic transport properties and conduction band offsets of asymmetric  $\text{InAs}/\text{In}_x\text{Ga}_{1-x}\text{As}/\text{GaAs}$  dot-in-well structures," *J. Phys. D: Appl. Phys.*, 45, 365104 (2012).
- [4] G. Vashisht, V. K. Dixit, S. Porwal, R. Kumar, T. K. Sharma and S. M. Oak, "Effect of charge carrier localization on the quantum efficiency and operating temperature range of  $\text{InAs}_x\text{P}_{1-x}/\text{InP}$  quantum well detectors," *J. Appl. Phys.*, 119, 095708 (2016).
- [5] V. K. Dixit, S. D. Singh, T. K. Sharma, Tapas Ganguli, Suparna Pal, B. Q. Khattak and S. M. Oak, "Studies on GaAs/AlGaAs based (p and n-type) quantum well infrared photodetector structures grown using metal organic vapour phase epitaxy," *IEEE Xplore*, 355, 9858874 (2008).
- [6] G. Vashisht, S. Halder, S. Porwal, R. Kumar, T. K. Sharma and V. K. Dixit, "InAsP/InP multiple quantum well based IR detectors with enhanced spectral photoresponse," XIX, IWPSD, IIT Delhi, Dec. 2017.
- [7] G. Vashisht, S. Porwal, R. Kumar, V. K. Dixit, T. K. Sharma, and S. M. Oak, "Development and application of InAsP/InP quantum well infrared detector," *AIP Conference Proceedings* 1731, 120033 (2016); <https://doi.org/10.1063/1.4948105>.
- [8] Q. Looker, M. G. Wood, P. W. Lake, J. K. Kim, and D. K. Serkland, "GaAs X-ray detectors with sub-nanosecond temporal response," *Review of Scientific Instruments* 90, 113505 (2019).
- [9] G. Lioliou, M. D. C. Whitaker, A.M. Barnett, "High temperature GaAs X-ray detectors," *J. Appl. Phys.*, 122, 244506 (2017).
- [10] G. Lioliou, A.M. Barnett, "Prototype GaAs X-ray detector and preamplifier electronics for a deep seabed mineral XRF spectrometer," *X-ray spectrometry*, 47, 201 (2018).
- [11] A. Owens, "Semiconductor materials and radiation detection," *J. Synchrotron Rad.* 13, 143 (2006).
- [12] A. Owens and A. Peacock, "Compound semiconductor radiation detectors," *Nuclear Instruments and Methods in Physics Research A* 531, 18 (2004).
- [13] P.J. Sellina and J. Vaitkus, "New materials for radiation hard semiconductor detectors," *Nuclear Instruments and Methods in Physics Research A*, 557, 479 (2006).
- [14] A. Chatterjee, S. K. Khamari, S. Porwal, S. Kher, and T. K. Sharma, "Effect of  $^{60}\text{Co}$   $\gamma$  irradiation on the nature of electron transport in highly n-type GaN based Schottky photodetectors," *J. Appl. Phys.*, 123, 161585 (2018).
- [15] A. Chatterjee, V. K. Agnihotri, S. K. Khamari, S. Porwal, A. Bose, S. C. Joshi, and T. K. Sharma, "Peculiarities of the current-voltage and capacitance-voltage characteristics of plasma etched GaN and their



- relevance to n-GaN Schottky photodetectors,” *J. Appl. Phys.*, 124, 104504 (2018).
- [16] A. Chatterjee, S. K. Khamari, S. Porwal, A. Bose and T. K. Sharma, “Influence of threading dislocations on the performance of GaN-based ultraviolet photodetectors,” *Proceedings of IWPSD, Kolkata, Dec. 2019.*
- [17] A. Chatterjee, S. K. Khamari, S. Porwal, and T. K. Sharma, “Role of ZrO<sub>2</sub> Passivation Layer Thickness in the Fabrication of High-Responsivity GaN Ultraviolet Photodetectors,” *Phys. Stat. Solidi RRL*, 13, 1900265 (2019).
- [18] A. Chatterjee, S. K. Khamari, S. Porwal and T. K. Sharma, “Impact of post deposition annealing of ZrO<sub>2</sub> insulating layer on the performance of GaN metal-semiconductor metal ultraviolet photodetectors,” *Proceedings of 4th IEEE-ICEE, Bangalore, Dec. 2018.*
- [19] A. Chatterjee, S. K. Khamari, S. Porwal and T. K. Sharma, “Effect of capacitance hysteresis on the performance of GaN metal-oxide-semiconductor photodetectors”, *Proceedings IWPSD, Delhi, Dec. 2017.*
- [20] C. Sharma, A. Khakha, G. Vashisht, A. Chatterjee, S. Porwal, S. K. Khamari, V. K. Dixit, T. K. Sharma and S.M. Oak, “Laser Beam Alignment Using Radiation Hard GaAs Quadrant *p-i-n* Photodetector,” *Proceedings of NLS, RRCAT, Indore, December 2015.*
- [21] H. Darji, G. Vashisht, R. Roychowdhury, S. Haldar, S. K. Khamari, V. K. Dixit, and T. K. Sharma, “Role of surface and interface states on the performance of GaAs based photodetectors,” *AIP Conference Proceedings* 2100, 020059 (2019); <https://doi.org/10.1063/1.5098613>.
- [22] V. K. Dixit, S. K. Khamari, A. Chatterjee, A. Khakha, T. K. Sharma and S. M. Oak, “Safety aspects in the fabrication of radiation hard semiconductor detectors,” *32 DAE Safety and Occupational Health Professionals Meet, RRCAT, October 2015.*
- [23] S. Haldar, G. Vashisht, U. K. Ghosh, A. K. Jaiswal, S. Porwal, A. Khakha, T. K. Sharma, and V. K. Dixit, “Development of a simple cost-effective maskless-photolithography system,” *AIP Conference Proceedings* 2115, 030219 (2019); <https://doi.org/10.1063/1.5113058>.
- [24] S. Haldar, “Magneto-optical transport studies on ultra-low disordered semiconductor quantum wells grown by MOVPE,” *PhD thesis, July 2020.*
- [25] P. Martyniuk, D. Benyahia, A. Kowalewski, L. Kubiszyn, D. Stepien, W. Gawron, and A. Rogalski, “Mid-wave T2SLs InAs/GaSb single pixel PIN detector with GaAs immersion lens for HOT condition,” *Solid-State Electronics*, 119, 1 (2016).
- [26] S. K. Khamari, S. Porwal, V. K. Dixit, T. K. Sharma, “Estimation of electron spin polarization from circularly polarized photoluminescence in strained quantum wells,” *J. Appl. Phys.*, 122, 025703 (2017).
- [27] V.K. Dixit, S. K. Khamari, S. Manwani, S. Porwal, K. Alexander, T. K. Sharma, S. Kher, S.M. Oak, “Effect of high dose gamma-ray irradiation on GaAs *p-i-n* photodetectors,” *Nuclear Instruments and Methods in Physics Research A* 785, 93 (2015).
- [28] V. R. V. Pillai, S. K. Khamari, V. K. Dixit, T. Ganguli, S. Kher, S. M. Oak, “Effect of Gamma-ray irradiation on breakdown voltage, ideality factor, dark current and series resistance of GaAs *p-i-n* diode,” *Nuclear Instruments and Methods in Physics Research A*, 685, 41 (2012).
- [29] S. K. Khamari, V. K. Dixit, T. Ganguli, S. Porwal, S.D. Singh, S. Kher, R.K. Sharma, S.M. Oak, “Effect of <sup>60</sup>Co Gamma-ray irradiation on electrical properties of GaAs epilayer and GaAs *p-i-n* diode,” *Nuclear Instruments and Methods in Physics Research Section B*, 269, 272 (2011).
- [30] G. Lioliou, and A.M. Barnett, “Gallium Arsenide detectors for X-ray and electron (beta particle) spectroscopy,” *Nuclear Instruments and Methods in Physics Research Section B* 336, 37 (2016).
- [31] G. Lioliou, S. Butera, S. Zhao, M.D.C Whitaker, A. M. Barnett, “GaAs Spectrometer for Planetary Electron Spectroscopy,” *Journal of Geophysical Research: Space Physics*, 123, 7568 (2018).
- [32] D. Pennicard, B. Pirard, O. Tolbanov, and K. Iniewski, “Semiconductor materials for X-ray Detectors,” *MRS BULLETIN*, 42 (2017).